Telecommunications and Radio Engineering 80(11):35–62 (2021)

PREDICTION OF RAIN-INDUCED ATTENUATION ALONG EARTH-SPACE LINKS AT MILLIMETER WAVE BANDS OVER WEST AFRICAN REGION

M.E. Sanyaolu,[1] O.F. Dairo,[1,2,*] A.O. Soge,[1] & A.A. Willoughby[1]

[1]*Department of Physical Sciences, Redeemer's University, Ede, Osun State, Nigeria*

[2]*Department of Electrical and Electronic Engineering, Redeemer's University, Ede, Osun State, Nigeria*

*Address all correspondence to: O.F. Dairo, Department of Electrical and Electronic Engineering, Redeemer's University, P.M.B. 230, Ede, Osun State, Nigeria; Tel.: +234-813-956-7700, E-mail: dairof@run.edu.ng

Original Manuscript Submitted: 10/14/2021; Final Draft Received: 1/16/2022

The present work characterizes the degree of rain-induced attenuation on 15–80 GHz earth-space communication links. Eutelsats 36B and 36C, and NigComSat-1R satellite links over five West African countries were considered through the International Telecommunication Union Radiocommunication Sector (ITU-R) [International Telecommunications Union (ITU)], Bryant, and Syjatogor rain attenuation models. Three locations were selected in each country for the analysis using 2013–2017 rain data obtained from the Global Precipitation Measurement (GPM) missions. ITU-R predicted higher attenuation values than the other two models; while Svjatogor values were close to ITU-R, and the Bryant model predicted the lowest. At 99.99% signal availability, rain attenuation along the earth-space link over the five countries ranged between 22.1 and 34.2 dB for Ku-band (15 GHz) but exceeded the satellites' link margins at Ka-band (30 GHz). At 0.1% unavailability, the range is 6–21 dB across all the locations for V-band (60 GHz), which implies that the satellites can sustain 99.9% of signal availability across the countries. However, for 99.99% and 99.9% signal availability at W-band, earth-space links can experience a total outage across the selected stations. Some locations in the northern parts can have 99% availability, which is an ~ 87 h/yr outage. Hence, the result could be a benchmark for planning trans-horizon radio communication links across West Africa.

KEY WORDS: *millimeter wave frequencies, radio propagation, rain attenuation, West Africa*

1. INTRODUCTION

The design of an excellent and effective satellite communication system requires good planning and reliable statistical data of associated radio meteorological parameters. The recent multiplicity of satellite communication systems implies that expanded bandwidth is required to accommodate more frequencies (Balal and Pinhasi, 2019; Fadilah and Pratama, 2018). As these high-frequency signals traverse the earth-space path length, they are prone to the effects of hydrometeors and various gases that distort their quality. The influence of these is primarily observed on the earth-space path links. Operating frequencies of > 10 GHz are largely impaired by rain attenuation as this results in fading

of signals (Yussuff and Khamis, 2014). For the design of the Ku to W frequency band, this impairment is a major inhibiting factor (Liolis et al., 2010) as free space is subject to attenuation by the effects of rain (Suriza et al., 2012). An electromagnetic wave impinging on raindrops is absorbed, scattered, or passed through, diminished in power, depending on the raindrop size and its distribution. The extent of loss experienced by such signals is determined by the intensity or rate of the rainfall (Upton et al., 2005). It has been deduced that the effects of rain attenuation vary from one region to another and that it increases as frequency increases (Choi et al., 1997). The attenuation, A, is related to the rain rate, R, by the following:

$$A = aR^b \tag{1}$$

where a and b are frequency-dependent regression coefficients. Equation (1) is especially true when the rainstorm is uniform along the path length.

The tropical climate of the West African subregion is largely characterized by heavy rainfall during the wet season monsoon months, from about April to October. The seasons are dictated by the north–south migration of the Inter-Tropical Convergence Zone, which either brings moist maritime air from the Gulf of Guinea, resulting in heavy rainfall as it is moving northward, or pushes down dry dusty continental air from the Sahara Desert when moving downward (Dairo and Kolawole, 2018). The rainfall pattern during these wet season months is usually heavy, with sizeable raindrops big enough to impair the signals (Ojo et al., 2008) as well as contribute to variability (Dairo and Kolawole, 2018). Consequently, it is essential to critically observe the level of signal degradation in this region to improve on the quality of service (Sanyaolu et al., 2020a), and more specifically, the precipitation associated with the monsoon, its advancement inland, and its precise timing (Lewis and Buontempo, 2016).

In this work, the prediction and verification of the impact of rain-induced attenuation on millimeter wave bands along earth-space satellite communication links in the West African subregion has been investigated using the NigComSat-1R (Nigeria), Eutelsat 36B and 36C satellites that beam down on this region.

2. REVIEW OF PREVIOUS WORKS

Copious research models have been recommended over the years for the estimation of fading along transmission of millimeter waves through the atmosphere right up to THz frequencies (Liebe, 1985, 1989; Allen et al., 1983; ITU, 2013). In fact, certain studies (Abdulrahman et al., 2012; Akobre et al., 2012; Omotosho et al., 2015) have investigated the effects of hydrometeors on time delay as well as attenuation using models that were developed. A core disadvantage of these empirical models is the paucity of data-

bases on microwave propagation measurements. Hence, the scarcity of rain data from the equatorial-tropical regions presents deviations in predictions when existing models from other regions are used or even deviate from direct measurements (Mandeep, 2009). In determining rain attenuation at a location, rain rate statistics at that location, i.e., measurement at a point, must be adhered to. This is because in convective precipitation, hop length may or may not exceed the dimensions of the raindrop, which makes point rate measurement a necessity.

Furthermore, polarization effects on the wave signal due to attenuation must be considered (Hogg et al., 1977), the reason being that waves polarized vertically are less susceptible to impairment than those horizontally polarized because of the oblate profile of the large raindrops. Consequently, different outage intervals for vertical and horizontal polarizations are usually observed on a hop. One way to avoid this inherent problem involving many hops is to introduce sequencing of polarization to equalize annual channel outage times. It has been argued (da Silva Mello et al., 2007) that the extrapolation method in the fourth equation of the International Telecommunications Union (ITU) ITU-RP.530-14 (ITU, 2012) is the major contributing weakness of the model. The downside of this method is because, with two regions experiencing same values of $A_{0.01}$ but different rain rate regimes, similar rain attenuation outcomes will be observed. Thus, to rectify this fault in the model, maximum rain rate distribution is introduced as an input to evaluate the cumulative distribution. Hence, this study employs three prediction models at different percentages of time with the rain rate.

3. METHODS AND DATA ANALYSES

3.1 Study Locations and Instrumentation

This study investigates the prediction and analysis of rain-induced attenuation on communication links over five West African countries, namely Benin, Cote d'Ivoire, Ghana, Nigeria, and Togo. The West African Sahel predominantly receives its rainfall during the northern hemisphere summer, which coincides with the Earth's aphelion passage. The rainfall distribution in time and space reflects circumstances peculiar to the whole of the West Africa subregion (Kouadio et al., 2011). The region's physical characteristics tend to weaken the rain-producing mechanisms (Adedokun, 1978; Biasutti, 2019). These mechanisms and the weather over the area are related to the interactions between the subtropical and its counterpart over the south Atlantic Ocean. These trends reflect the harmattan characteristics and the south westerly airstreams associated with the two high-pressure centers (Acheampong, 1987).

In Nigeria, the climate is largely tropical, seasonally damp, and humid, from Guinea in the south through the central Savanna to the north's Sahel. The annual rainfall is < 500 mm in the far northeast, typically ranging from 450 to 1,050 mm, 1050 to 1400 mm, to 1400 to 2700 mm in the Sahelian, Savanna, and Guinean climates, respectively (Ogungbenro and Morakinyo, 2014). The location of Nigeria is between latitudes 4° N and 14° N.

Togo is associated with a tropical climate situated in the Sahara's southern region, characterized by dry and rainy seasons due to the African monsoon, which commences mid-April to October in the south and May to October in the north, with a marked decrease in rainfall along the coast from July to September.

The latitude and longitude of Benin vary between 6° N to 13° N and 0° E to 4° E, respectively. The climate is typically humid and hot, with average annual precipitation of 1,360 mm, like other Guinean coasts in West Africa. The dry season is associated with the winter. Although the rainy season is due to the African monsoon, it stretches in the far north from May to September and from mid-March to October in the south.

Ghana is characterized by the tropical climate, ranging from warm, dry, and humid in the Guinean zone to semi-arid in the northern Sahel. Ghana's location in the Gulf of Guinea, just above the Equator, is bounded between latitudes 4° N and 11° N and longitudes 3° W and 1° E. Typical average annual precipitation ranges between ~ 8×10^2 and 2×10^3 mm from the Sahel in the north to the south's Guinean coast.

Cote d'Ivoire is a typically dry tropical climate; the temperature ranges between 28 and 37°C, with 12×10^2 mm of annual rainfall. Four seasons characterize this climatic region, including the rainy season from April to mid-July laden with frequent rain and thunderstorms, and the dry season from mid-July to September.

Nigeria launched its Communication Satellite-1 (NigComSat-1R) on May 13, 2007, placed at 42° E in a geostationary orbit, with an estimated service life of 15 yr. For each location sampled in Nigeria, the elevation and azimuth angles for the links to NigComSat-1R were determined. On the other hand, with 52.5° dish elevation, 256.4° azimuth (magnetic compass), and 69.0° polarization, Eutelsat 36B co-located with Eutelsat 36C at 36° E orbital position are the leading providers of direct-to-home (DTH) broadcasting services in West Africa. The Eutelsat 36B and 36C satellites were launched on November 24, 2009, and December 24, 2015, respectively. The magnetic compass was used to determine the elevation angle for the remaining locations understudy.

This study considered three locations in each country, as shown in Fig. 1. The locations' characteristics are presented in Table 1, while Table 2 shows the geographical factors for rain attenuation prediction using the ITU-R models at the sites.

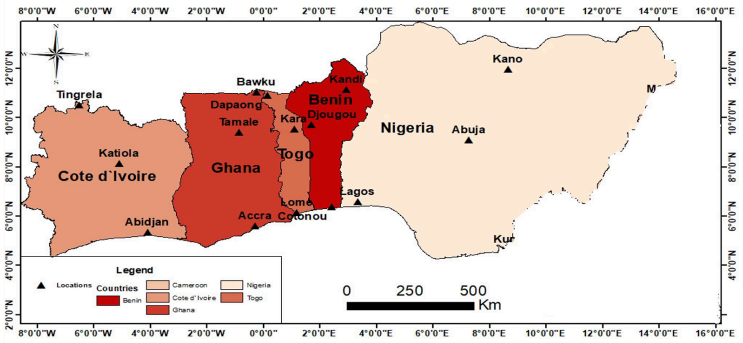

FIG. 1: Map of 5 West African countries used for this study

TABLE 1: Site characteristics of study locations

Countries	Location	Longitude (+°*E* or –°*W*)	Latitude (°*N*)	$R_{0.01}$	Height above sea level (m)	Elevation angle (Θ)	Average annual rainfall (mm)
Togo	Dapaong	0.1208	10.9100	112.0153	298.1	57.9	1690.84
	Kara	1.0858	9.5566	121.7667	315.6	56.6	2238.91
	Lome	1.1627	6.1507	98.0607	20.3	52.5	1080.8
Ghana	Bawku	–0.2534	11.0464	115.802	247.6	57.9	1890.9
	Tamale	–0.8631	9.4031	111.8454	191.2	56.1	1682.23
	Accra	–0.3028	5.6243	95.61596	91.9	51.8	992.807
Benin	Kandi	2.9250	11.1372	111.8021	170.6	57.9	1680.04
	Djougou	1.6824	9.7355	120.1067	44.9	56.6	2137.89
	Cotonou	2.3985	6.3802	111.5723	5.5	52.5	1668.45
Nigeria	Kano	8.6455	11.9820	93.62148	448.4	63.3	1374.56
	Abuja	7.2744	9.1094	101.0583	478.1	58.2	2427.931
	Lagos	3.3475	6.5869	110.7246	32.2	53.3	2498.43
Cote d'Ivoire	Tingrela	–6. 5215	10.5204	120.6235	362.5	57.1	2168.99
	Katiola	–5.12057	8.1464	114.3649	291.8	54.9	1813.12
	Abidjan	–4.0976	5.3619	113.7375	76.0	52.2	1779.88

TABLE 2: Geometrical factors of communication links at 0.01% unavailability using the ITU R model[1]

						Horizontal L_E (km) at f (GHz)			
Country	**Location**	h_r	h_s	L_s	L_G	**Ku (f = 15)**	**Ka (f = 30)**	**V (f = 60)**	**W (f = 80)**
Togo	Dapaong	4.50	0.290	5.25	2.79	3.04	3.65	4.54	5.00
	Kara	4.85	0.310	12.01	6.61	4.33	5.52	7.41	8.39
	Lome	4.85	0.020	5.64	3.43	3.26	3.89	4.86	5.36
Ghana	Bawku	4.50	0.240	7.07	4.14	3.60	4.45	5.78	6.45
	Tamale	4.50	0.190	5.19	2.89	2.97	3.56	4.47	4.94
	Accra	4.85	0.090	6.05	3.74	3.29	3.91	4.87	5.37
Benin	Kandi	4.85	0.171	5.04	2.58	3.10	3.58	4.30	4.67
	Djougou	4.85	0.441	5.25	2.86	3.21	3.21	4.02	4.42
	Cotonou	4.80	0.051	5.57	3.02	2.53	3.15	4.16	5.07
Nigeria	Kano	4.77	0.566	4.77	2.25	3.02	3.90	5.10	5.66
	Abuja	4.80	0.152	5.12	2.15	3.18	4.17	5.50	6.12
	Lagos	4.80	0.019	5.26	2.01	3.67	5.19	6.00	6.80
Cote d'Ivoire	Tingrela	4.84	0.360	5.33	2.89	2.73	3.32	4.21	4.66
	Katiola	4.84	0.290	5.51	3.18	2.87	3.47	4.39	4.86
	Abidjan	4.50	0.076	6.04	3.70	3.02	3.64	4.63	5.14

[1] L_s is slant-path length (km), h_s is antenna height (km), h_r is rain height, L_G is horizontal projection, L_E is effective path length (km), and f is frequency (GHz).

Five-year rainfall parameters obtained from the GPM mission's Core Observatory, spanning 2013–2017, were used for this study. The GPM is an international U.S./Japanese Earth science satellite mission with NASA and JAXA's prime agencies, respectively. Specifically, the GPM was designed to unify precipitation measurements made by the GPM core satellite along with a constellation of partner satellites. The GPM Core Observatory satellite is at an altitude of 407 km in a non-Sun-synchronous orbit that covers the Earth from 65° S to 65° N—from the Antarctic Circle to the Arctic Circle. GPM provides a four-dimensional view of rain, snow, sleet, and storms from space. The GPM constellation of satellites can observe precipitation over the entire globe every 2–3 h (Krishna et al., 2017).

3.2 Rain Rate Model

A technique for translating the available rainfall data to the corresponding one-minute rain rate cumulative distribution (CD) would be beneficial for radio wave engineers. For this reason, using the refined Moupfouma model and long-term mean annual rainfall data, the one-minute rain rate CD can be calculated.

Several studies have shown that the one-minute rain rate distribution in tropical regions can best be represented by the Moupfouma model with refined parameters (Ojo et al., 2008, 2009; Mandeep, 2009; Abdulrahman et al., 2012). Moupfouma discovered that the CD of the one-minute rain rate could be formalized as follows:

$$P\,(R \geq r) = \frac{1}{10^4}\left[R_{0.01}(r+1)^{-1}\right]^b \exp\left[\mu\,(R_{0.01} - r)\right] \tag{2a}$$

where

$$b = \left[\frac{r}{R_{0.01}} - 1\right]\ln\left[1 + \frac{1+r}{R_{0.01}}\right]$$

The cumulative rain distribution slope is governed by μ, which is a function of the local atmospheric conditions and geographic topography. For tropical and subtropical regions

$$\mu = \frac{4\ln 10}{R_{0.01}} \exp\left[-\lambda\left(\frac{r}{R_{0.01}}\right)^{\gamma}\right] \tag{2b}$$

where λ and γ are positive coefficients, such that λ = 1.066 and γ = 0.214, and $R_{0.01}$ is the rain rate exceeded for 0.01% of the time. $R_{0.01}$ is obtained using the Chebil and Rahman (1999) model. Thus, the refined Moupfouma model can determine the one-minute rain rate cumulative distribution from the long-term mean annual rainfall rate. For the estimation of $R_{0.01}$ from the long-term mean annual precipitation M, several techniques were identified. These include the Morita (1978), Ghosh et al. (2012), Ito and Hosoya (1999, 2006), Ito et al. (1999), Ajayi and Ofoche (1984), regression tropical India, and Chebil and Rahman models. All the five models used the power-law relationship (Chebil and Rahman, 1999; Ojo et al., 2008).

$$R_{0.01} = \alpha M^{\beta} \tag{3}$$

where α and β are regression coefficients, which are 12.2903 and 0.2973, respectively. M is the total rainfall measured for a year, and $R_{0.01}$ the rain rate measured in millimeters per hour. On the basis of the measured one-minute rain rate CD at several locations in Malaysia, Singapore, and Indonesia, these models were compared and the Chebil model was found suitable for the tropical regions (Moupfouma and Martin, 1995; Ajayi et al., 1996; Shrestha and Choi, 2017; Islam et al., 2018; Ojo et al., 2009; Obiyemi et al., 2014; Igwe et al., 2019; Sanyaolu et al., 2020b). Hence, the rain rate, $R_{0.01}$, for this study has been deduced using the Chebil and Rahman model and is presented in Table 1.

3.3 Rain Attenuation Prediction Models

Rain attenuation can either be obtained directly from microwave link measurements or estimated from the rain rate and rain drop-size distribution data, according to Ajayi and Barbaliscia (1990). Researchers have developed various methods for calculating CDs of attenuation due to rain from rain intensity measurements (COST, 1996; ITU, 2015). Among the well-utilized rain attenuation models, the ITU-R, Bryant, and Svjatogor models have been found suitable for the tropical regions, mainly for a region where direct measurements are not available (Shrestha and Choi, 2017; Igwe, 2019; Sanyaolu et al., 2020b). The step-by-step computation using the models is presented in Sections 3.3.1–3.3.3.

3.3.1 ITU-R Model

ITU-RP.838-3 (ITU, 2005) specified that the specific attenuation γ_R (measured in decibels per kilometer) is obtained from the rain rate R (measured in millimeters per hour) using the power-law relationship, as follows:

$$\gamma_R = kR^{\alpha} \tag{4}$$

where the values for the coefficients k and α are determined as functions of frequency, f (measured in gigahertz), in the range of $1–10 \times 10^2$ GHz, from the following equations, which have been developed from curve-fitting to power-law coefficients derived from scattering calculations:

$$\log_{10} k = \sum_{j=1}^{4} \left\{ a_j \exp\left[-\left(\frac{\log_{10} f - b_j}{c_j} \right)^2 \right] \right\} + m_k \log_{10} f + c_k \tag{5}$$

$$\alpha = \sum_{j=1}^{5} \left\{ a_j \exp\left[-\left(\frac{\log_{10} f - b_j}{c_j} \right)^2 \right] \right\} + m_\alpha \log_{10} f + c_\alpha \tag{6}$$

For horizontal polarization, the constants are written as k_H and α_H (ITU, 2005).

ITU-RP.618-13 (ITU, 2017) used an effective path length to consider the time–space variability of rain intensity along the terrestrial path. Rain attenuation exceeded for the year's 0.01% time is calculated from the average one-minute rain intensity exceeded at the same time percentage.

The estimated attenuation to be exceeded for other time percentages of an average year, in the range of 0.001–5%, is determined from the attenuation to be exceeded for 0.01% for an average year. The step-by-step procedure of computing the model is as follows:

$$L_s = \frac{(h_r - h_s)}{\sin\theta} \tag{7}$$

For $\theta < 5°$, the following formula is used:

$$L_s = \frac{2(h_r - h_s)}{\left(\sin^2\theta + \frac{2(h_r - h_s)}{R_e}\right)^{1/2} + \sin\theta} \tag{8}$$

The horizontal projection, L_G, of the slantpath length is obtained using

$$L_G = L_s \cos\theta \tag{9}$$

The rain rate at 0.01% is

$$R_{0.01} = \alpha M^{\beta} \tag{10}$$

where α and β are regression coefficients and are defined as α = 12.2903 and β = 0.2973.

The specific attenuation, γ_R, is expressed as follows:

$$\gamma_R = K(R_{0.01})^{\alpha} \tag{11}$$

The horizontal reduction factor, $r_{0.01}$, for 0.01% of the time is as follows:

$$r_{0.01} = \left[1 + 0.78\left(\frac{L_G\,\gamma_R}{f}\right)^{1/2} - 0.38\left(1 - \frac{1}{e^{2L_G}}\right)\right]^{-1} \tag{12}$$

The vertical adjustment factor, $v_{0.01}$, for 0.01% of the time is as follows:

$$\zeta = \tan^{-1}[(h_r - h_s)(L_G\, r_{0.01})^{-1}] \tag{13}$$

For $\zeta > \theta$, $L_R = (L_G\, r_{0.01})(\cos\theta)^{-1}$.
Else, $L_R = (h_r - h_s)(\sin\theta)^{-1}$.
If $|\varphi| < 36°$, then $x = 36 - |\varphi|$.
Else, $x = 0$.

$$V_{0.01} = \left[1 + \sqrt{\sin\theta}\left(31\left\{1 - e^{-(\theta/(1+x))}\right\}\right)(L_R\gamma_R)^{1/2} f^{-2} - 0.45\right]^{-1} \tag{14}$$

The effective path length is

$$L_E = L_R v_{0.01} \tag{15}$$

The 0.01% of annual average attenuation exceeded is computed using the following:

$$A_{0.01} = \gamma_R L_E \tag{16}$$

For other percentages, ranging from 0.001 to 5%, the annual average predicted attenuation to be exceeded is obtained from 0.01% of the annual average, as follows:

If $p \geq 1\%$ or $|\varphi| \geq 36°$, then $\beta = 0$

If $p < 1\%$ and $|\varphi| < 36°$ and $\theta \geq 25°$

then $\beta = -0.005(|\varphi|) - 36$; otherwise, $\beta = -0.005\,(|\varphi| - 36) + 1.8 - 4.25 \sin\theta$.

$$A_p = A_{0.01}\left(100p\right)^{-\left(0.655 + 0.033\ln(p) - 0.045\ln(A_{0.01}) - \beta(1-p)\sin\theta\right)} \tag{17}$$

where

$$B = \begin{Bmatrix} 0 & \text{if } p \geq 1\% \text{ or } |\varphi| \geq 36° \\ -0.005\left(|\varphi| - 36°\right) & \text{if } p \leq 1\% \text{ and } |\varphi| < 36° \text{ and } \theta \geq 25° \\ -0.005\left(|\varphi| - 36°\right) + 1.8 - 4.25\sin\theta & \text{otherwise} \end{Bmatrix}$$

3.3.2 Bryant Model

The Bryant model employs the concept of effective rain cell and variable rain height to calculate the distribution of rain attenuation (Bryant et al., 2001). The steps involved in this model are as follows (Hanif et al., 2013):

Step 1: The path length–to–Rain–cell (PR) parameter:

$$PR = 1 + 2L\,(\pi D)^{-1} \tag{18}$$

where the rain cell diameter, D, is given by

$$D = \frac{5.40 \times 10^2}{R_p^{12}} \tag{19}$$

and the horizontal projection, L, is expressed as follows:

$$L = H_{\mathrm{r}}(\tan \theta)^{-1} \tag{20}$$

Step 2: The rain height, H_{r}

$$H_{\mathrm{r}} = \frac{4.5 \times 10^4 + 5\ R_{\mathrm{P}}^{1.65}}{10000} \tag{21}$$

Step 3: The slant path attenuation, A_{s}, is given as follows:

$$A_{\mathrm{s}} = 1.57 D_m \mathrm{K}_n \gamma_p \frac{L_{\mathrm{s}}}{\xi L + D} \tag{22}$$

where L_{S} is the slant-path length, γ_p is the specific attenuation (measured in decibels per kilometer)

$$D_m = \left(\frac{2}{\pi}\right) D \tag{23}$$

k_n is the number of cells and expressed as follows:

$$k_n = \exp(0.007R_p) \tag{24}$$

$$\xi = \frac{1}{\sqrt{2}}\exp(\sin\theta) \text{ for } \theta \leq 55^\circ \tag{25}$$

$$\xi = 1.1 \tan\theta \text{ for } \theta > 55^\circ \tag{26}$$

3.3.3 Svjatogor Model

The Svjatogor model (Svjatogor, 1985) defines its effective rain height, H_r, depending on the rain intensity as follows:

$$H_r = 2.7[\log_{10}(0.3R_p + 1.5)]^{-1} + 1.5 \times 10^{-3} R\text{p} \tag{27}$$

The path length reduction factor is formulated in the following:

$$K_{rs} = e^{Y};\ Y = -4.5\times10^{-3} R_p^{0.68}\left[\frac{H_r}{\tan(\theta)}\right]^{0.6} \tag{28}$$

The rain attenuation A_s is given as follows:

$$A_s = kR_p^{\infty} L_s K_{rs} \tag{29}$$

where

$$L_s = \frac{(H_r - H_s)}{\sin\theta} \quad \text{for } \theta \geq 5° \tag{30}$$

and

$$L_s = \frac{2(H_r - H_s)}{\left[\sin^2\theta + \frac{2(H_r - H_s)}{R_e}\right]^{0.5} + \sin\theta} \quad \text{for } \theta < 5° \tag{31}$$

$R_e = 85 \times 10^2$ km (effective radius of the earth).

4. RESULT AND DISCUSSION

This section presents the results obtained from using the study locations data. The link margin of NigComSat-1R over the Atlantic Ocean region is 20 dB; whereas, it is ~ 27 dB for Eutelsat 36B and 37C. The implication is that the devices used could tolerate a further 20 and 27 dB attenuation between the transmitter and the receiver.

4.1 Monthly Rain Distribution

Figure 2 is the monthly average of rainfall accumulation based on five years (January 2013 to December 2017) of rainfall data obtained from the GPM mission's Core Observatory. The monthly rainfall distribution for the observation period shows the different monthly peaks across all the locations, which invariably revealed the worst months of rain attenuations at these locations. For example, all the stations in Nigeria recorded their peaks in August. Lagos recorded the highest rainfall out of the three stations, with a peak monthly average rainfall accumulation of 511 mm, followed by Kano and Abuja with 484 and 473 mm, respectively.

Similarly, Bawku and Tamale in Ghana recorded their peak monthly average rainfall accumulation in August with about 561 and 457 mm, respectively, while Accra recorded its peak in June with about 189 mm. In the Benin Republic, Djougou and Kandi have their peaks in August and July with about 582 and 390 mm, respectively. On the average in Togo, Lome has the lowest average rainfall accumulation. However, Lome recorded the highest values of about 128 and 296 mm in March and May, respectively, compared to Bawku and Kara. The July pattern of rainfall distribution is similar to that of August in Togo, where Dapaong and Kara recorded their peaks in August with about 409 and 541 mm, respectively. In Cote d'Ivoire, Tingrela recorded its highest monthly average

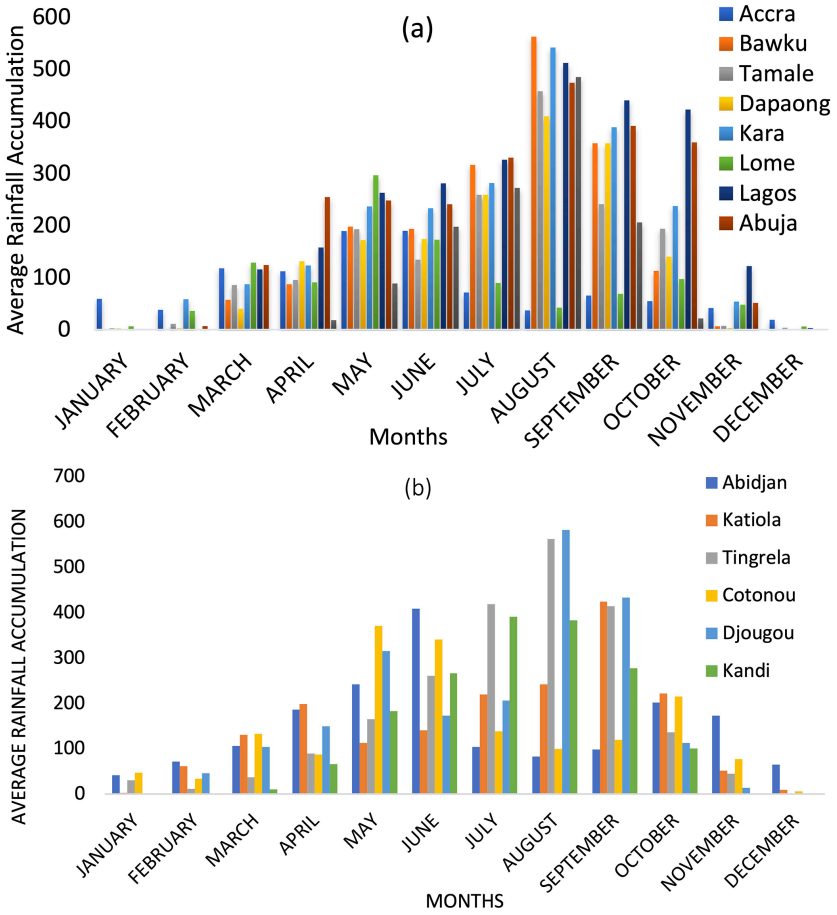

FIG. 2: Five years monthly average rainfall accumulation in (a) Ghana, Togo, and Nigeria and (b) Benin and Cote d'Ivoire

rainfall accumulation with about 562 mm in August, which is second behind Djougou across the five West African countries under consideration. The Katiola and Abidjan peaks, 424 and 408 mm, were in September and June, respectively.

4.2 Cumulative Distribution of Rain Rate

Predicted rain rate cumulative distributions for all location are shown in Table 3. The rain rate data were estimated using the Moupfouma one-minute integration model and presented in millimeters per hour. The estimated rainfall intensity ranged from 0.001 to 1% exceedance. At 0.001%, Nigeria recorded the highest rain rate of 185 mm/h in Lagos. On the other hand, Ghana, Cote d'Ivoire, Togo, and Benin recorded the highest rain rates of 162, 146, 198, and 155 mm in Bawku, Abidjan, Dapaong, and Djougou, respectively.

TABLE 3: Cumulative distribution of rain rate (in millimeters per hour) across all study locations

Countries and cities		Percentage exceedance							
		0.001	**0.01**	**0.03**	**0.05**	**0.1**	**0.3**	**0.5**	**1**
Nigeria	Kano	185	110	97	89	71	60	50	15
	Lagos	170	101	94	78	62	54	44	13
	Abuja	160	102	93	66	51	44	33	12
Ghana	Bawku	162	115	113	101	83	61	56	19
	Tamale	144	111	102	91	73	52	48	16
	Accra	137	95	92	80	66	50	41	14
Cote d'Ivoire	Abidjan	146	113	106	88	70	65	41	16
	Katiola	145	114	101	79	66	54	38	15
	Tingrela	135	120	85	63	50	41	23	12
Togo	Lome	145	101	98	84	70	51	28	17
	Kara	180	121	110	98	82	58	30	17
	Dapaong	198	112	118	105	90	73	43	19
Benin	Cotonou	147	111	102	87	60	43	28	16
	Kandi	115	101	67	55	57	35	25	13
	Djougou	155	120	83	66	52	30	30	15

The patterns of all distributions have a similar trend across all the locations under study. Hence, rain attenuation is considered rain-rate dependent. However, rain-rate data exceeding radio signal availability is what most radio engineers and planners need for designing radio networks, because higher rain rates lead to increased losses of high-frequency radio signals.

The CD function (CDF) of the measured rain rate in Nigeria is shown in Fig. 3. The CDF revealed the highest distribution pattern in Lagos, followed by Abuja. The observed distribution in Lagos is primarily due to its coastal location along the Gulf of

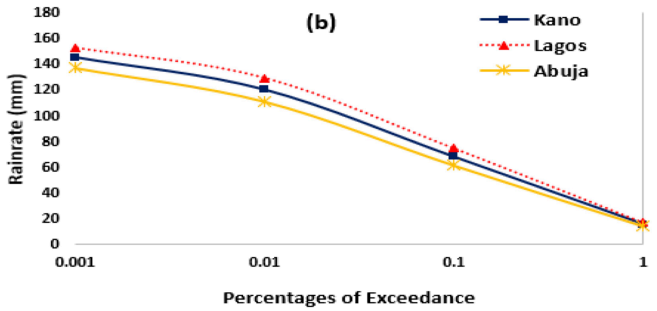

FIG. 3: Cumulative distribution of rain rate based on measurement data conducted at the studied locations in Nigeria

Guinea in Nigeria, where frequent and high rainfall occurs, which could be due to the conventional type of rain. The lowest pattern is observed in Kano.

4.3 Rain Attenuation

A typical result of the comparison of the measured and predicted rain attenuation is shown in Fig. 4. The measured data are only presented for a typical location (Nigeria) due to the availability of measured attenuation data. The results revealed that the ITU-R model predicted higher attenuation values at higher availability time compared to the measured rain attenuation.

Rain attenuation and the effective path length were also calculated for frequencies ranging from 6 to 100 GHz for rain rates exceeded 0.01% of times; the results are presented in Fig. 5. Generally, the result shows that rain attenuation increases with increasing frequency. The attenuation was very low at 6 and 12 GHz but increased as the frequency increases, and attenuation became very pronounced at 100 GHz. At 0.01%, predicted attenuations for the C- to W-band, using ITU-R, were between 5 and 200 dB in Accra, Ghana, while 3 and 145 dB were recorded in Kano, Nigeria. For Tingrela in Cote d'Ivoire, the range was 4–192 dB.

In Nigeria, Lagos has the highest attenuation, followed by Abuja and Kano. It was observed that rain attenuation is less severe in the northern part but more severe in the south. On the other hand, Bawku recorded the highest attenuation in Ghana while Kara recorded higher attenuation in Togo than both Dapaong and Lome. The results also suggest that there could be a total outage of signals at 0.01% unavailability across Ka-, V-, and W-bands for all elevation angles in all 18 locations during rainfall, i.e., link unavailability of > 53 min of outage in a year.

Eutelsat plays a leading role among the operators of DTH broadcasting in Sub-Saharan Africa and uses antenna pointing characteristics of 52.5° dish elevation, 256.4° (magnetic compass) azimuth, and 69.0° polarization. The magnetic compass is used to determine the elevation angle for each of the locations. NigComSat-1R was used to determine the elevation angle for locations in Nigeria, as presented in Table 1.

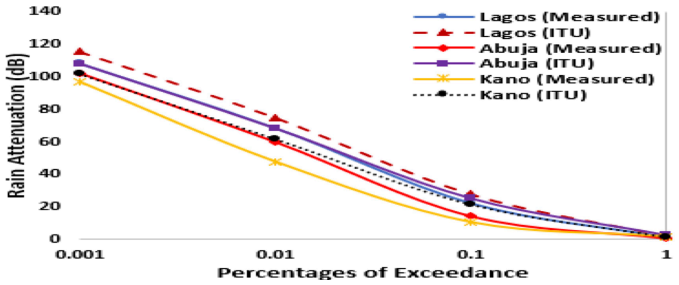

FIG. 4: Comparison of the measured and predicted rain attenuation in Nigeria

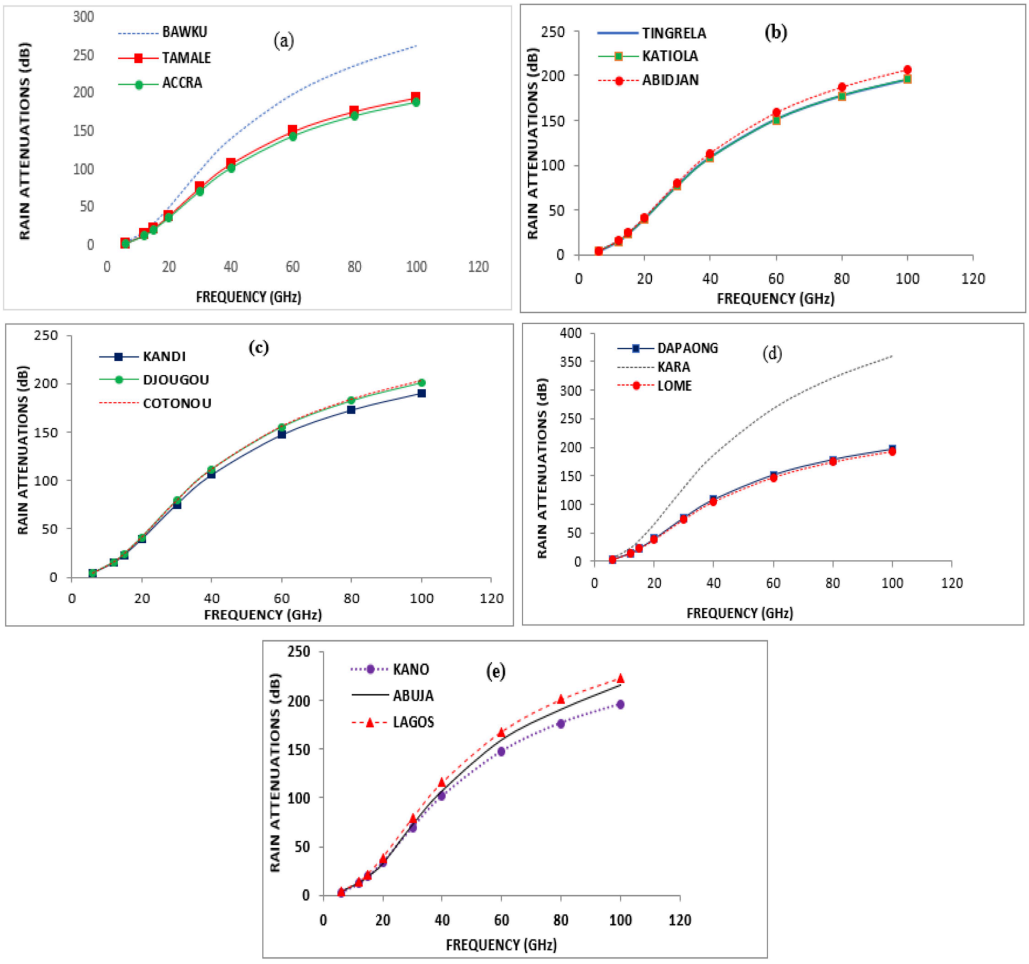

FIG. 5: Attenuation at 0.01% exceedance for C-W bands in (a) Ghana, (b) Cote d'Ivoire, (c) Benin, (d) Togo, and (e) Nigeria

Figures 6–9 show rain attenuation cumulative distribution for downlink frequencies of both NigComSat-1R and Eutelsat Hot Bird 13B with a very small aperture terminal (VSAT) at Ku (15 GHz), Ka- (30 GHz), V- (60 GHz), and W-band (80 GHz) covering West Africa. The ITU-R model is the most widely accepted estimation method of rain attenuation on satellite communication networks all over the world. Therefore, for reliability, existing models are compared to it.

Figure 6 shows the cumulative rain attenuation distribution for the downlink frequency of Ku (15 GHz), from 0.001 to 1 percentage of exceedance. The 0.01% exceedance is equivalent to signal unavailability of ~ 53 min in a year, which is an equivalent of ~ 8.7 s outage per day (Omotosho and Oluwafemi, 2009). The Svjatogor model predictions closely agree with the ITU-R model; whereas, the Bryant model underestimated the

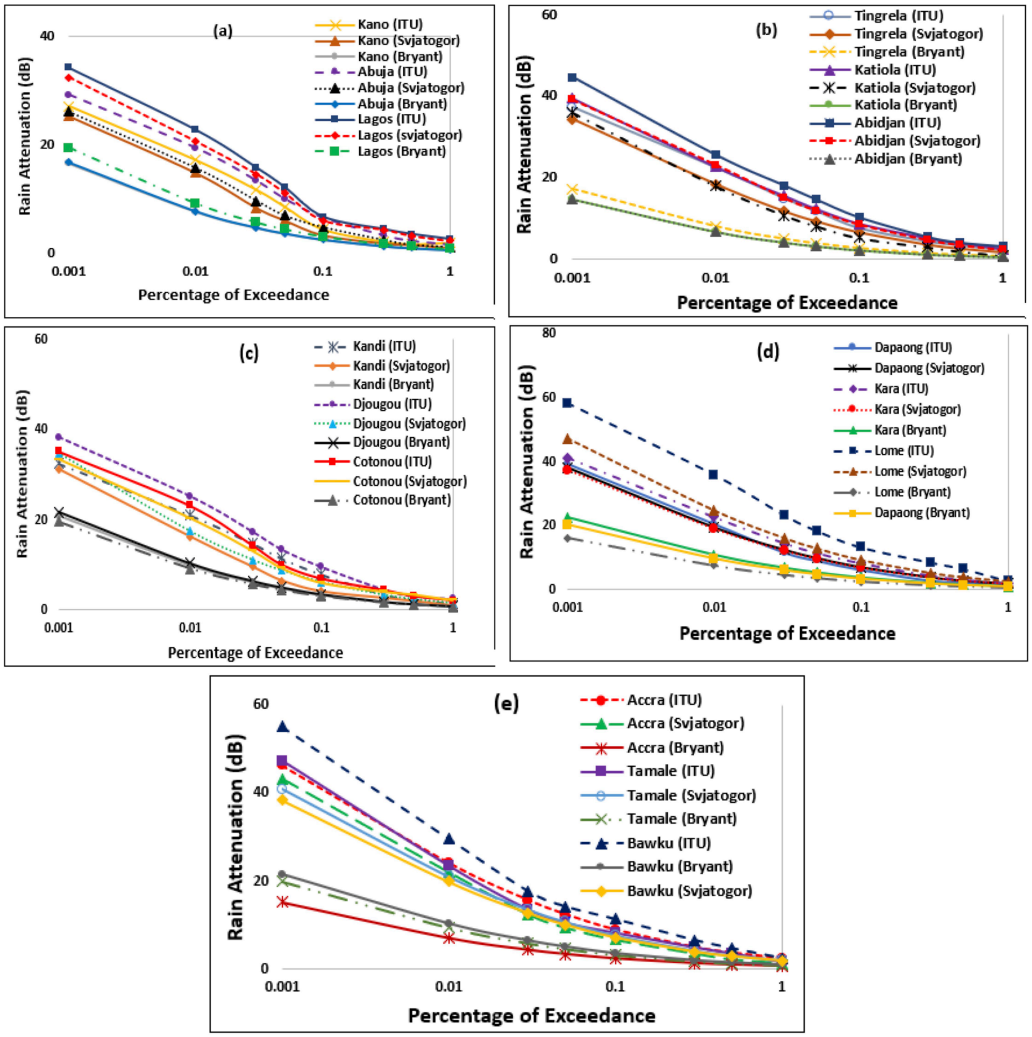

FIG. 6: Rain attenuation distribution at Ku-band (15 GHz) frequency in (a) Nigeria, (b) Cote d'Ivoire, (c) Benin, (d) Togo, and (e) Ghana

rain attenuation values. For instance, the rain attenuation predicted by the ITU-R model for 0.001% exceedance probability is 27.1 dB and 29.3 dB for Kano and Abuja, respectively, and 34.2 dB for Lagos. Concurrently, the Svjatogor model predicted 25.2, 26.1, and 32.2 dB for Kano, Abuja, and Lagos, respectively. In comparison, the Bryant model predicted 16.4, 16.6, and 19.4 dB for Kano, Abuja, and Lagos, respectively. Lagos has the highest attenuation in Nigeria. In Cote d'Ivoire, the ITU-R model prediction showed that rain attenuation ranges from 25.2 to 20.1 dB with Abidjan having the highest rain attenuation. On the other hand, the Svjatogor model predicted within the range of 18–23 dB and Bryant predicted between 17–14 dB for the selected locations in Cote d'Ivoire.

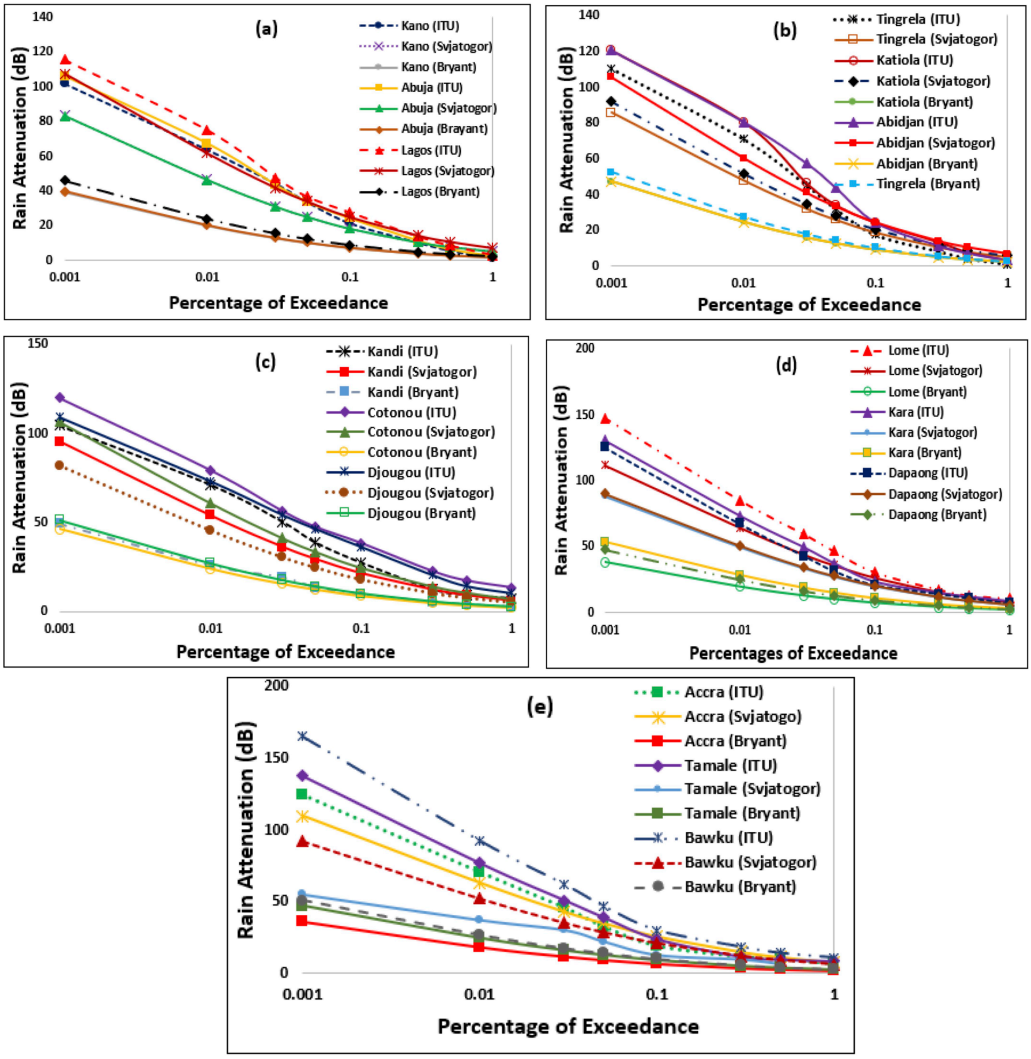

FIG. 7: Cumulative distributions of rain attenuation distribution at Ka-band (30 GHz) frequency in (a) Nigeria, (b) Cote d'Ivoire, (c) Benin, (d) Togo, and (e) Ghana

According to ITU-R prediction, Djougou recorded the highest rain attenuation in the Benin Republic with 25.2 dB, followed by Cotonou and Kandi having 24.1 and 22.8 dB, respectively. The Svjatogor model predictions show an overlap of Djougou and Cotonou at 0.001% unavailability with 33.3 dB. The Bryant model underestimated all locations having 16, 10.1, and 9.2 dB in Kandi, Djougou, and Cotonou, respectively. Generally, the ITU-R predicted higher at all sites. However, the predictions of the other two models closely followed the trend of ITU-R though Bryant's were much lower at the exceedance percentage of time considered across all the stations. In Togo, the rain attenuation ranges between 25.1 and 22.3 dB with Lome having the highest signal loss.

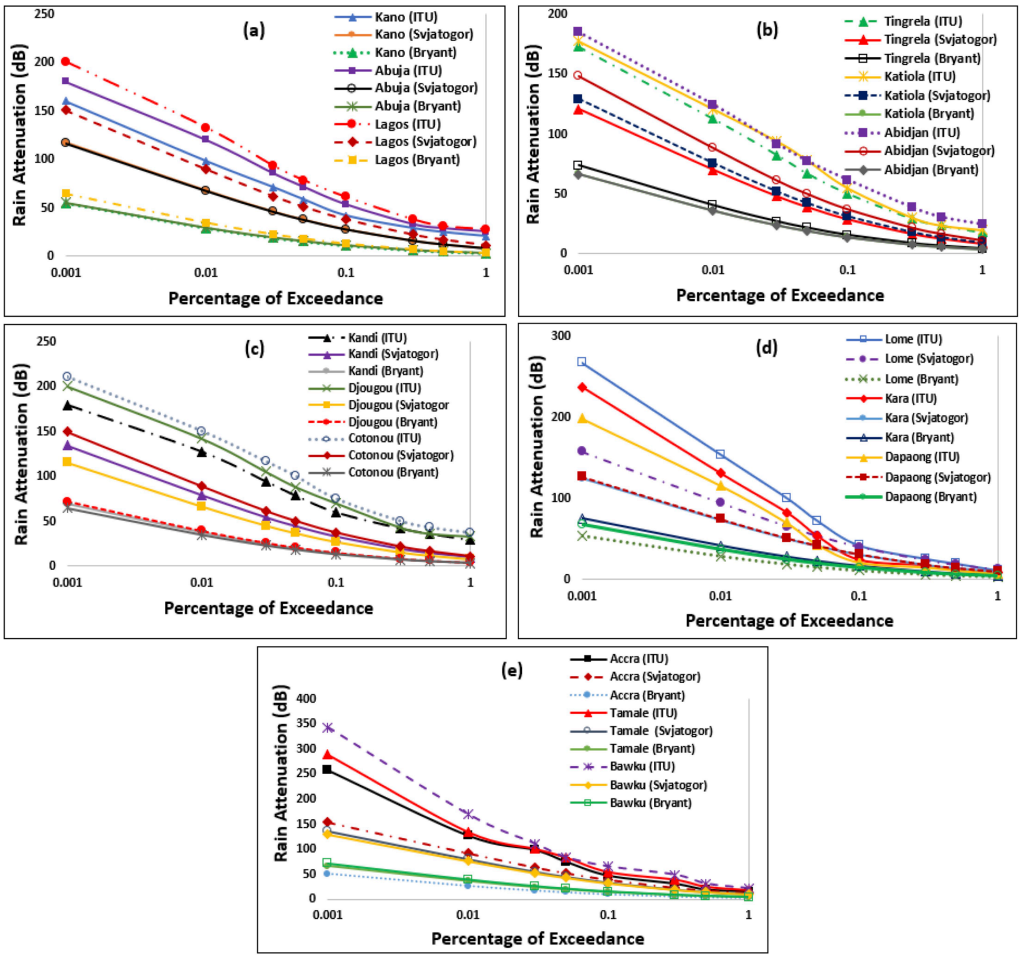

FIG. 8: Rain attenuation distribution at V-band (60 GHz) frequency in (a) Nigeria, (b) Cote d'Ivoire, (c) Benin, (d) Togo, and (e) Ghana

In contrast, Bawku has the highest attenuation in Ghana, which corresponds to the same location with the highest average rainfall accumulation.

Generally, the result also revealed that 99.99% signal availability is not attainable, as rain attenuation for all the five countries ranges between 22.1 and 34.2 dB, which could be more than the link margins of both Eutelsat 13 and NigComSat-1R at specific locations. The attenuation range across the study locations exceeded the specified link margin of NigComSat-1R values but below that of Eutelsat at some sites. On the other hand, Akinwumi et al. (2016) related the attenuation range to the EIRP. In particular, NigComSat-1R signal fading will be noticeable at the Ku-band for 0.01% exceedance. In Singapore, for an equatorial and tropical region, like Nigeria, Ku-band measurements with INTELSAT VI at 11 GHz show a rain attenuation range of 2 to 15 dB (Timothy et al., 2000).

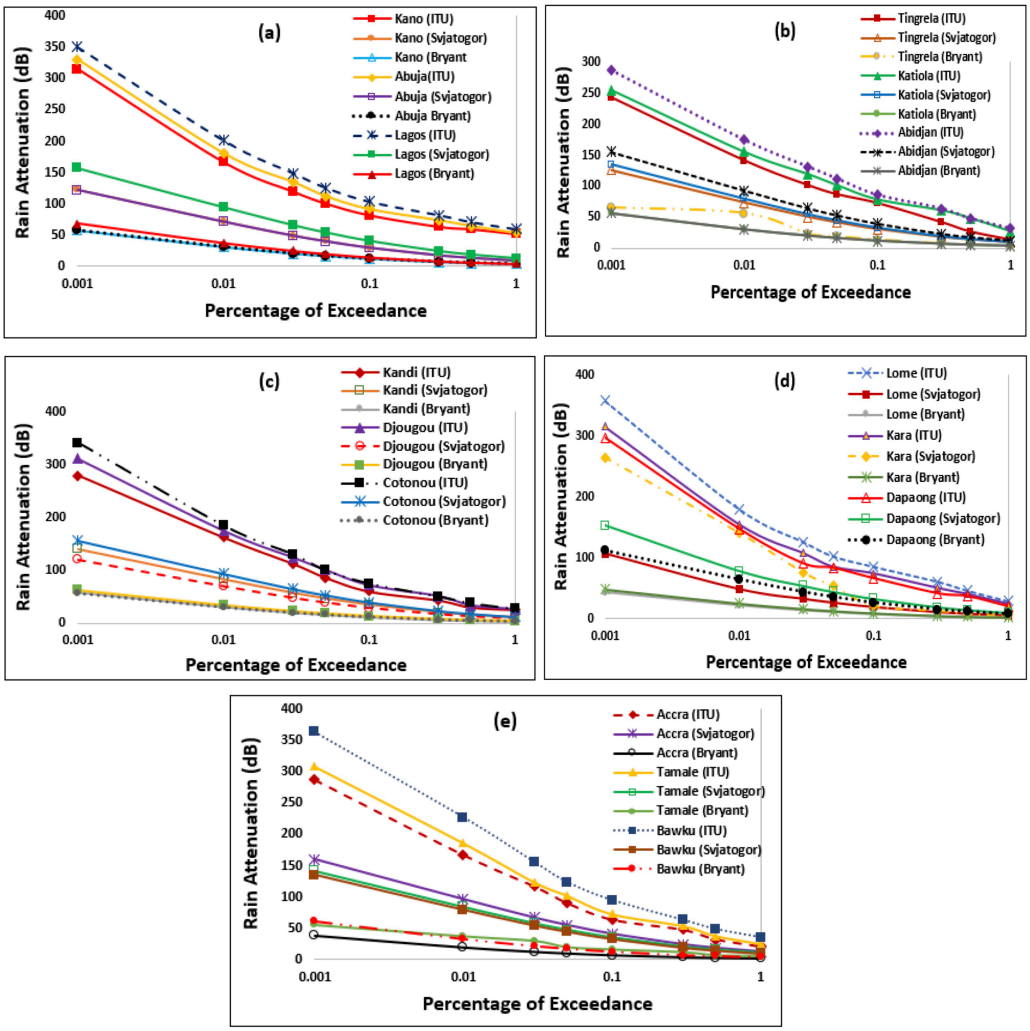

FIG. 9: Rain attenuation distribution at V-band (80 GHz) frequency in (a) Nigeria, (b) Cote d'Ivoire, (c) Benin, (d) Togo, and (e) Ghana

At Ka-band downlink frequency (30 GHz) and 99.99% signal availability, Fig. 7 shows that all the study locations will experience attenuation due to rain because the values exceeded both satellites' link margins. Also, rain attenuation was more prevalent along the coast, except for Djougou in the Benin Republic, which recorded higher attenuation values than its remaining locations. At 0.01% of unavailability, Lagos, Nigeria recorded the highest attenuation of ~ 74 dB, ranging from 74 to 79 dB in Cote d'Ivoire. Ranges of 61–71 dB, 67–87 dB, and 70–83 dB were recorded for Benin, Togo, and Ghana, respectively. The results agree with the frequent severe fading observed in an equatorial climate, such as in Malaysia, at 38 GHz with values typically up to 46 dB for 99.99% (Badron et al., 2010).

However, at 0.1 of unavailability (which amounts to 525.6 min of signal loss in a year), the rain attenuation level of all studied locations ranges between 6 and 21 dB, which indicates that a radio signal of 99.9% availability will not suffer undue attenuation from bad weather. The rain attenuation experiments with ACTS Satellite (VSATS) were conducted in the U.S. for a 10-year duration at Ka-band, using the beacon receivers. The study showed that rain attenuation exceeds 20 dB for 99.9% of a typical year at the Ka-band (27.5 GHz) under moderate elevation angles. Fading is worse for higher rainfall climates in the U.S. (Roberto, 1997). Hence, the results obtained at Ka-band in this study for tropical climate are in order.

Figure 8 shows the results of all the locations at V-band (60 GHz). These frequencies are currently engaged in the deployment of both 5G mobile and satellite networks. The results show that there is pronounced rain attenuation at this millimeter wave across the five countries. The implication is there will be signal outage due to rainfall at 0.01% unavailability, where Nigeria recorded a range of 98–122 dB, while the recorded ranges of 112–129, 127–141, and 126–169 dB are for Cote d'Ivoire, Benin, and Ghana, respectively. At 99.9% availability, even Togo, with the least rain attenuation range of 20.3–28.4 dB, is not guaranteed of no signal degradation. On the other hand, nearly all the locations will experience 99% availability since none of the sites recorded attenuation above 20 dB at 1% unavailability. The V-band can utilize mitigation techniques such as adaptive coding and power to reduce the fading effect.

At W-band (80 GHz) frequency, Fig. 9 shows that, at 0.01 percentage unavailability of signals, rain attenuation in Nigeria ranges from 166 to 200 dB, where Lagos recorded the highest attenuation value, which corresponds to the highest rain intensity in Nigeria, followed by Abuja and Kano. Abidjan, Katiola, and Tingrela in Cote d'Ivoire recorded about 173, 140, and 154 dB, respectively. Generally, the ranges of rain attenuation recorded were 162–184, 157–186, and 166–207 dB for Benin, Togo, and Ghana, respectively.

Though W-band is a future spectrum, the present study is needed to plan for any possible impairment. Both 99.99 and 99.9% of signal availabilities are not feasible at this frequency. However, some locations in the northern parts, such as Bawku in Ghana, Dapaong in Togo, and Tingrela in Cote d'Ivoire, would have 99% signal availability. At this frequency band, the availability represents ~ 87.6 h of outage in a year.

5. CONCLUSION

This paper has provided information on rain-induced attenuation on communication links at Ku-W bands in the West Africa region. The ITU-R model was compared to the Svjator and Bryant models. The result showed that ITU-R predicted higher than the two models and Bryant prediction were much lower than ITU-R and Svjatogor. The monthly rainfall pattern over the region, which indicates the worst months at which radio signals may be unavailable, has been presented. The results obtained showed that the attenuation increases from C-band to W-band. This work further revealed the possibilities of system availability and unavailability at different percentages of times of the year. For

instance, at 15 GHz, 99.99% of signal availability is possible across all locations on NigComSat-1R and Eutelsat.

Similarly, at 30 GHz, only 99.9% availabilities can be sustained while at 60 GHz and 99.9%, only Togo can tolerate the attenuation level, while other locations will experience a total signal outage. Also, at 80 GHz, both 99.99 and 99.9% of signal availabilities are not feasible at all the selected frequencies. However, some locations in the northern parts, such as Bawku in Ghana, Dapaong in Togo, and Tingrela in Cote d'Ivoire, can experience 99% of signals availability. This study has provided crucial technical information to the International Telecommunications Union (ITU) for frequency allocation and system designers and link-budgeting in the West African zone.

ACKNOWLEDGMENTS

The authors thank the National Aeronautics and Space Administration (NASA) and Centre for Basic Space Science (CBSS) for their support to access the data used for this study. The anonymous reviewers and Olumide Julius Ademuyiwa are also much appreciated.

REFERENCES

Abdulrahman, A.Y., Rahman, T.A., Rahim, S.K.A., Islam, M.R., and Abdulrahman, M.K.A., Rain Attenuation Predictions on Terrestrial Radio Links: Differential Equations Approach, *Trans. Emerg. Telecommun. Technol.*, vol. **23**, pp. 293–301, 2012.

Acheampong, P.K., Rainfall Characteristics over the West African Sahel-The Nigerian Example, *Singap. J. Trop. Geogr.*, vol. **8**, no. 2, pp. 72–83, 1987.

Adedokun, J.A., West African Precipitation and Dominant Atmospheric Mechanisms, *Arch. Met. Geoph. Biokl.*, vol. **A27**, pp. 289–310, 1978.

Ajayi, G.O. and Ofoche, E.B.C., Some Tropical Rainfall Rate Characteristics at ILE-IFE for Microwave and Millimeter Wave Applications, *J. Appl. Meteorol. Climatol.*, vol. **23**, no. 4, pp. 562–567, 1984.

Ajayi, G.O. and Barbaliscia, F., Prediction of Attenuation Due to Rain: Characteristics of the 0°C Isotherm in Temperate and Tropical Climates, *Int. J. Satell. Commun. Netw.*, vol. **8**, no. 3, pp. 187–196, 1990.

Ajayi, G.O., Feng, S., Radicella, S.M., and Reddy, B.M., *Handbook on Radio Propagation Related to Satellite Communication in Tropical and Subtropical Countries*, Trieste, Italy: ICTP, pp. 7–14, 1996.

Akinwumi, S.A., Omotosho, T., Usikalu, M.R., Adewusi, M.O., and Ometan, O.O., Atmospheric Gases Attenuation in West Africa, *2016 IEEE Radio and Antenna Days of the Indian Ocean*, New York: IEEE, 2016.

Akobre, S.K., Diawuo, K., and Gyasi-Agyei, A., Weather Effects on Ku Band Digital Satellite Television System in Kumasi, *IEEE 4th Int. Conf. on Adaptive Science Technology*, New York: IEEE, pp. 12–16, 2012.

Allen, K.C., Liebe, H.J., and Rush, C.M., Estimates of Millimeter Wave Attenuation for 18 United States Cities, NTIA Rep. No. 83–119, Natl. Telecommun. and Information Admin., Boulder, CO, pp. 83–119, 1983.

Badron, K., Ismail, A.F., Din, J., and Tharek, A.R., Rain Induced Attenuation Studies for V-Band Satellite Communication in Tropical Region, *J. Atmos. Sol. Terr. Phys.*, vol. **73**, nos. 5–6, pp. 601–610, 2010.

Balal, Y. and Pinhasi, Y., Atmospheric Effects on Millimeter and Sub-Millimeter (THz) Satellite Communication Paths, *J. Infrared Millim. Terahertz Waves*, vol. **40**, pp. 219–230, 2019.

Biasutti, M., Rainfall Trends in the African Sahel: Characteristics, Processes, and Causes, *WIREs Clim. Change*, vol **10**, pp. 1–22, 2019.

Bryant, G.H., Adimula, I., Riva, C., and Brussaard, G., Rain Attenuation Statistics from Rain Cell Diameters and Heights, *Int. J. Satell. Commun.*, vol. **19**, no. 3, pp. 263–283, 2001.

Chebil, J. and Rahman, T.A., Rain Rate Statistical Conversion for the Prediction of Rain Attenuation in Malaysia, *Electron. Lett.*, vol. **35**, no. 12, pp. 1019–1021, 1999.

Choi, Y.S., Lee, J.H., and Kim, J.M., Rain Attenuation Measurements of the Korea Sat Beacon Signal on 12 GHz, *Proc. of CLIMPARA '98*, Ottawa, Canada: Union Radio Scientifique Internationale (URSI), pp. 208–211, 1997.

COST, Radiowave Propagation Effects on Next Generation Fixed Services Terrestrial Telecommunications Systems, COST 235, Final Report, European Commission Directorate-General XIII, Office for Official Publications of the European Communities, Luxembourg, 1996.

Dairo, O.F. and Kolawole, L.B., Radio Refractivity Gradients in the Lowest 100 m of the Atmosphere over Lagos, Nigeria in the Rainy-Harmattan Transition Phase, *J. Atmos. Sol. Terr. Phys.*, vol. **167**, pp. 169–176, 2018.

da Silva Mello, L.A.R, Pontes, M.S., de Souza, R.M., and Perez Garcia, N.A., Prediction of Rain Attenuation in Terrestrial Links Using Full Rainfall Rate Distribution, *Electron. Lett.*, vol. **43**, no. 25, pp. 1442–1443, 2007.

Fadilah, N. and Pratama, R., Comparison of Rain Attenuation Estimation in IGH Frequency in Indonesia Region for LAPAN Communication Satellite, *J. Phys. Conf. Ser.*, vol. **1130**, p. 012036, 2018.

Ghosh, K., Bhattacharya, P.P., and Das, P.K., Effect of Multipath Fading and Propagation Environment on the Performance of a Fermat Point Based Energy Efficient Geocast Routing Protocol, *Int. J. Wirel. Mobile Netw.*, vol. **4**, no. 1, pp. 215–224, 2012.

Hanif, M.N.N., Lee, C.H., Arman, M., and Mandeep, J.S., Analysis of Rain Attenuation Model for Ku Band in Cameron Highland, Malaysia, *Proc. of 13th Int. Conf. on Applied Informatics and Communications*, pp. 287–290, 2013.

Hogg, D.C., Giger, A.J., Longton, A.C., and Muller, E.E., The Influence of Rain on Design of 11-GHz Terrestrial Radio Relay, *Bell Syst. Tech. J.*, vol. **56**, no. 9, pp. 575–1580, 1977.

Igwe, K.C., Oyedum, O.D., Ajewole, M.O., and Aibinu, A.M., Evaluation of Some Rain Attenuation Prediction Models for Satellite Communication at Ku and Ka Bands, *J. Atmos. Sol. Terr. Phys.*, vol. **188**, pp. 52–61, 2019.

Islam, R., Alam, M., Lwas, A.K., and Mohamad, S., Rain Rate Distributions for Microwave Link Design Based on Long Term Measurement in Malaysia, *Indones. J. Electr. Eng. Comput. Sci.*, vol. **10**, no. 3, pp. 1023–1029, 2018.

Ito, C. and Hosoya, Y., Proposal of a Global Conversion Method for Different Integration Time Rain Rates by Using M Distribution and Regional Climatic Parameters, *Electr. Commun. Jpn. Part I*, vol. **89**, no. 4, pp. 1–9, 2006.

Ito, C. and Hosaya, Y., Worldwide 1-Min. Rain Rate Distribution Prediction Method which Uses Thunderstorm Ratio as Regional Climatic Parameter, *Electron. Lett.*, vol. **35**, no. 18, pp. 1585–1587, 1999.

Ito, C., Hosoya, Y., and Kashiwa, T., A Proposed Prediction Method for the Worldwide One-Minute Rain Rate Distribution, *Trans. Inst. Electron. Inf. Commun. Eng. B-II (Jpn.)*, vol. **35**, no. 18, pp. 1585–1587, 1999 (in Japanese).

ITU, Specific Attenuation Model for Rain for Use in Prediction Methods, ITU-R P.838-3, ITU, Geneva, Switzerland, 2005.

ITU, Propagation Data and Prediction Methods Required for the Design of Terrestrial Line-of-Sight Systems, ITU-R P.530-14, ITU, Geneva, Switzerland, 2012.

ITU, Attenuation Due to Clouds and Fog, ITU-R P.840-6, ITU, Geneva, Switzerland, 2013.

ITU, Propagation Data and Prediction Methods Required for the Design of Earth–Space Telecommunication Systems, ITU-R P.618–8, ITU, Geneva, Switzerland, 2015.

ITU, Propagation Data and Prediction Methods Required for the Eesign of Earth-Space Telecommunication Systems, ITU-R P.618-13, ITU, Geneva, Switzerland, 2017.

Kouadio, K.Y., Aman, A., Ochou, A.D., Ali, K.E., and Assamoi, P.A., Rainfall Variability Patterns in West Africa: Case of Cote d'Ivoire and Ghana, *J. Environ. Sci. Eng.*, vol. **5**, pp. 1229–1238, 2011.

Krishna, U.V.M., Das, S.K., Deshpande, S.M., Doiphode, S.L., and Pandithurai, G., The Assessment of Global Precipitation Measurement Estimates over the Indian Subcontinent, *Earth Space Sci.*, vol. **4**, pp. 540–553, 2017.

Lewis, K. and Buontempo, C., *Climate Impacts in the Sahel and West Africa: The Role of Climate Science in Policy Making*, West African Papers, No. 02, Paris: OECD Publishing, 2016.

Liebe, H.J., An Updated Model for Millimeter Wave Propagation in Moist Air, *Radio Sci.*, vol. **20**, no. 5, pp. 1069–1089, 1985.

Liebe, H.J., MPM-An Atmospheric Millimeter-Wave Propagation Model, *Int. J. Infrared Millim. Waves*, vol. **10**, no. 6, pp. 631–650, 1989.

Liolis, K.P., Panagopoulos, A.D., and Scalise, S., Combination of Tropospheric and Local Environment Effects for Mobile Satellite Systems Above 10 GHz, *IEEE Trans. Veh. Technol.*, vol. **59**, no. 3, pp. 1109–1120, 2010.

Mandeep, J.S., Slant Path Rain Attenuation Comparison of Prediction Models for Satellite Applications in Malaysia, *J. Geophys. Res.*, vol. **114**, no. D17, pp. 1–12, 2009.

Morita, K., A Method for Estimating All Season and Heavy Rain Season Rain Rate Distribution, *ECL Tech. J.*, vol. **27**, no. 10, pp. 2249–2266, 1978 (in Japanese).

Moupfouma, F. and Martin, L., Modelling of the Rainfall Rate Cumulative Distribution for the Design of Satellite and Terrestrial Communication Systems, *Int. J. Sat. Commun.*, vol. **13**, pp. 105–115, 1995.

Obiyemi, O.O., Ibiyemi, T.S., and Akande, S.O., Rainfall Variability and Impact on Communication Infrastructure in Nigeria, *J. Telecommun.*, vol. **25**, no. 1, pp. 6–11, 2014.

Ogungbenro, B.S. and Morakinyo, T.E., Rainfall Distribution and Change Detection across Climatic Zones in Nigeria, *Weather Clim. Extremes*, vols. **5–6**, pp. 1–6, 2014.

Ojo, J.S., Ajewole, M.O., and Emiliani, L.D., One-Minute Rain-Rate Contour Maps for Microwave-Communication-System Planning in a Tropical Country: Nigeria, *IEEE Antennas Propag. Mag.*, vol. **51**, pp. 82–89, 2009.

Ojo, J.S., Ajewole, M.O., and Sarkar, S.K., Rain Rate and Rain Attenuation Prediction for Satellite Communication in Ku and Ka Bands over Nigeria, *Prog. Electromagn. Res. B*, vol. **5**, pp. 207–223, 2008.

Omotosho, T.V. and Oluwafemi, C.O., Impairment of Radio Wave Signal by Rainfall on Fixed Satellite Service on Earth–Space Path at 37 Stations in Nigeria, *J. Atmos. Sol. Terr. Phys.*, vol. **71**, nos. 8–9, pp. 830–840, 2009.

Omotosho, T.V., Obiyemi, O.O., Mandeep, J.S., Abdullah, M., Akinwumi, S.A., Willoughby, A.A., Ometan, O.O., and Adewusi, M.O., Review of Rain Attenuation Measurements on Earth and Space Links in Nigeria, *IEEE 2015 Int. Conf. Space Sci. Commun. (IconSpace)*, Langkawi, Malaysia, pp. 42–46, 2015.

Roberto, J.A., Rain Fade Compensation Alternatives for Ka-Band Communication Satellite, *Third Ka-Band Utilization Conf.*, Sorrento, Italy, 1997.

Sanyaolu, M.E., Dairo, O.F., Willoughby, A.A., and Kolawole, L.B., Estimation of Rain Fade Durations on Communication Links at Ka-Band in Equatorial and Tropical Regions, *Telecommun. Radio Eng.*, vol. **79**, no. 2, pp. 129–141, 2020a.

Sanyaolu, M.E., Dairo, O.F., Willoughby, A.A., and Kolawole, L.B., 1-Minute Rain Rate Distribution for Communication Link Design Based on Ground and Satellite Measurements in West Africa, *Telecommun. Radio Eng.*, vol. **79**, no. 6, pp. 533–543, 2020b.

Shrestha, S. and Choi, D.Y., Rain Attenuation Statistics over Millimeter Wave Bands in South Korea, *J. Atmos. Sol. Terr. Phys.*, vol. **152**, pp. 1–10, 2017.

Suriza, A.Z., Rafiqul, I.M., Wajdi, A.K., and Naji, A.W., Proposed Parameters of Specific Rain Attenuation Prediction for Free Space Optics Link Operating in Tropical Region, *J. Atmos. Sol. Terr. Phys.*, vol. **94**, pp. 93–99, 2012.

Svjatogor, L., Prostranstvennaia Korelacia Vypadenjija Dozdjej Vdol Zemnoj Po-Verchnostji, Symp. Expertov Stran Uchastnic Programmy INTERKOSMOS (Interkosmos Symp., Theme 5 of the Established Telecommunication Working Group, Dresden, GDR, 1985 (in Russian).

Timothy, K.I., Ong, J.T., and Choo, E.B.L, Descriptive Fade Slope Statistics on INTELSAT Ku-Band Communication Link, *Electron. Lett.*, vol. **36**, no. 20, pp. 1733–1734, 2000.

Upton, G.J.P., Holt, A.R. Cummings, R.J., Rahimi, A.R., and Goddard, J.W.F., Microwave Links: The Future for Urban Rainfall Measurement, *Atmos. Res.*, vol. **77**, nos. 1–4, pp. 300–312, 2005.

Yussuff, A.I. and Khamis, N.H.H., Rain Attenuation Prediction Model for Lagos at Millimeter Wave Bands, *J. Atmos. Ocean. Technol*., vol. **31**, no. 3, pp. 639–646, 2014.